Zeeman splitting of interacting two-dimensional electrons with two effective masses

K. Vakili, E. Tutuc, and M. Shayegan
Department of Electrical Engineering, Princeton University, Princeton, NJ 08544
(Dated: February 6, 2008)

We have realized an AlAs two-dimensional electron system in which electrons occupy conduction-band valleys with different Fermi contours and effective masses. In the quantum Hall regime, we observe both resistivity spikes and persistent gaps at crossings between the Landau levels originating from these two valleys. From the positions of the spikes in tilted magnetic field and measurements of the energy gaps away from the crossings, we find that, after occupation of the minority valley, the spin susceptibility drops rapidly, and the electrons possess a *single* interaction-enhanced g-factor, despite the dissimilarity of the two occupied valleys.

PACS numbers: 73.21.Fg, 73.43.-f, 73.43.Qt, 73.61.Ey

Coincidences between Landau levels (LLs) in multi-component quantum Hall systems provide information regarding the relative energy scales of the two-dimensional electron system (2DES). For example, coincidences between LLs with different spin occur when the ratio of Zeeman and cyclotron energies is an integer, yielding the product of the interaction renormalized effective mass (m^*) and Landè g-factor (g^*) which is proportional to the spin susceptibility of the system [1]. To date, most studies of LL crossings have been conducted in systems wherein the discrete components (e.g. two layers in a symmetric bilayer) are very similar [2]. Here, we report the realization of a 2DES in which electrons occupy two very dissimilar valleys, exhibiting different Fermi contours and effective masses. We study inter-valley LL crossings in this system, manifested by resistivity spikes, and extract information about the relative energy scales of the two valleys. We find that g^*m^* drops rapidly upon occupation of the minority valley and, remarkably, that the electrons possess a single g^* despite the dissimilarity of the two occupied valleys.

Aluminum Arsenide (AlAs) is a practical system to study crossings between LLs originating from different valleys thanks to the degree of control that exists over valley occupation in this material. Bulk AlAs has three conduction band minima at the X-points of the Brillouin zone, each leading to an ellipsoidal Fermi surface with a longitudinal mass of $m_l = 1.04$ and transverse masses of $m_t = 0.21$ [3], in units of the vacuum electron mass. Though confinement along the [001] axis lowers the energy of the valley oriented out of the plane (Z) with respect to the two in-plane valleys (X and Y), the strain caused by lattice mismatch between the AlAs quantum well (QW) and the GaAs substrate on which it is grown has the opposite effect. Consequently, there is a crossover between Z and (X,Y) valley occupation at a threshold QW thickness of $\simeq 55$ Å [4, 5]. By studying a QW near this thickness, we sought to simultaneously occupy the Z valley and either the X or Y valley [6]. The former has an isotropic Fermi contour projection in the plane of the 2DES with a band effective cyclotron mass of $m_t = 0.21$, while the latter each have an anisotropic Fermi contour with cyclotron mass of $(m_l m_t)^{1/2} = 0.47$. This is similar to another system studied previously [7], except there the occupied valleys were separated in different parallel layers while the present system has both within a single 2DES.

We studied two samples (A and B) from the same wafer, each containing a 50 Å AlAs QW flanked by $Al_{0.4}Ga_{0.6}As$ barriers and modulation doped with Si. They were patterned in an L-shaped Hall bar configuration oriented parallel to the in-plane crystal axes. Ohmic contacts were made by depositing AuGeNi and alloying in a reducing environment. We also deposited metallic front and back gates to allow for control of the electron density, n. The samples were cooled in a pumped ^{3}He refrigerator with a base temperature of 0.3 K that was equipped with a single-axis rotating stage to allow for *in situ* variation of the angle, θ, of the magnetic field, B, with respect to the sample normal. We define $B_\perp$ as the component of B perpendicular to the 2DES plane.

To demonstrate the novel behavior of g^*m^* and g^* in this system, particularly the equality of the g^* values when the two valleys are occupied, it is first necessary to identify the LL crossings and deduce the energy level diagram. In Fig. 1(a), we show longitudinal resistivity (ρ_{xx}) vs. B at $\theta = 0^o$ in sample A as n increases from 4.0 (top) to 5.6 x 10^{11} cm^{-2} (bottom). Only the Z valley is occupied for low values of n, as evidenced by the isotropy of ρ_{xx} and by comparison of measured g^*m^* with values reported in Ref. [8] where only the Z valley is occupied in a very narrow (45 Å-wide) QW [Fig. 2]. At low n, Shubnikov-de Haas (SdH) oscillations persist down to $B_\perp \simeq 0.5$ T. As n increases, however, the onset of SdH oscillations moves to higher $B_\perp$, eventually exceeding 2 T, and ρ_{xx} spikes become evident in the quantum Hall minima (e.g. around $\nu = 3$). Both of these observations can be associated with the population of a second valley, which must be one of the in-plane valleys (we will refer to it as X) [9]. As the X valley becomes populated, the commingling of its LLs with those of the Z valley at low $B_\perp$ reduces the size of all energy gaps and produces

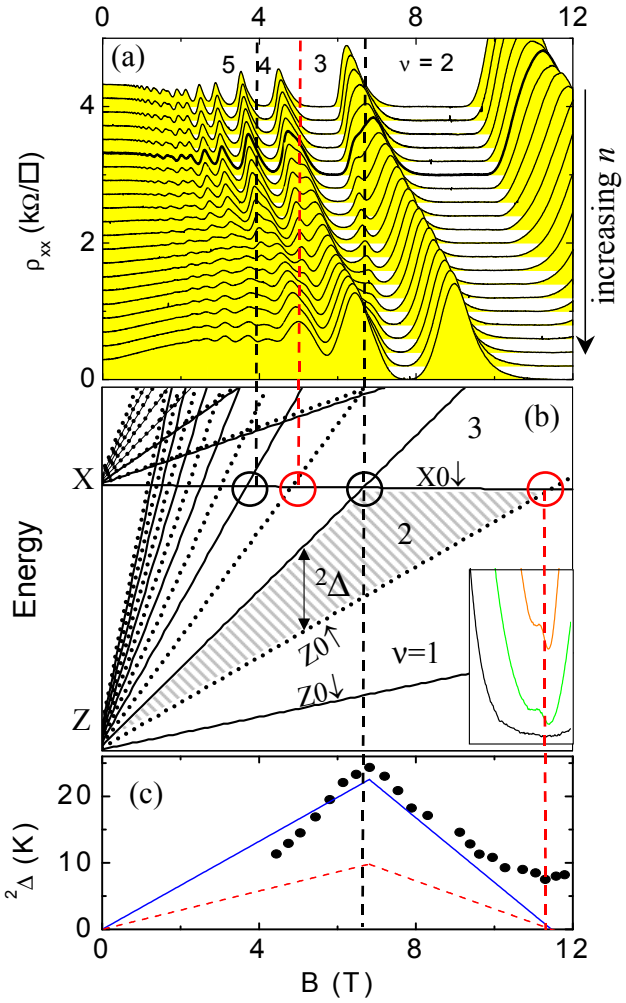

FIG. 1: (color online) (a) ρ_{xx} vs. $B_\perp$ at $\theta = 0$ for n between 4.0 (top) and 5.6 x 10^{11} cm^{-2} (bottom) in sample A, at $T =$ 0.3 K. The trace at the onset of X-valley population ($n = n_V =$ 4.2 x 10^{11} cm^{-2}) is shown as bold. Traces are vertically offset for clarity. (b) The energy level "fan" diagram corresponding to the data shown in (a), with the Z and X valley LLs labeled and the relevant LL crossings circled (black for same-spin and red for opposite-spin crossings). The $\nu = 2$ energy gap ($^2\Delta$) is shaded, and the units of the vertical axis are arbitrary. The inset of (b) shows ρ_{xx} vs. $B_\perp$ at $n = 5.5$ x 10^{11} cm^{-2} near ν = 2 [plotted on the same horizontal scale as (a) and (c)] for T = 0.3 K (black), 0.95 K (green), and 1.1 K (orange). (c) $^2\Delta$ vs. $B_\perp$ as n is varied from 2.1 to 5.7 x 10 ^{11} cm^{-2}. The solid blue and dashed red curves are the predictions for $^2\Delta$ based on the fan diagram of (b) if all of the enhancement of g^*m^* is assigned to g^* or to m^* respectively.

the observed shift of SdH onset to higher $B_\perp$, where the gaps are larger. The spikes, then, can be associated with crossings that occur between LLs originating from the X and Z valleys.

This can be shown by considering the energy level (fan) diagram. The expression for the energy of a LL is:

$$E = (N + \frac{1}{2})\hbar\omega_c \pm \frac{1}{2}g^*\mu_B B \pm \frac{1}{2}\Delta_V \qquad (1)$$

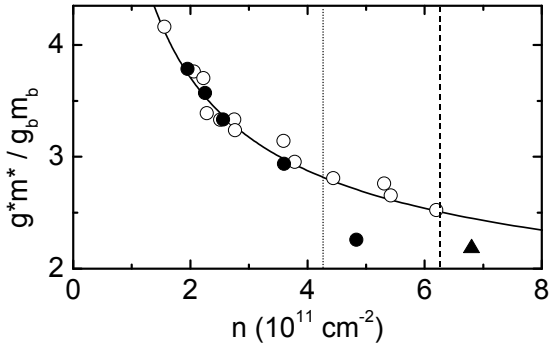

FIG. 2: The enhancement of g^*m^* over the band value measured in sample A (filled circles) and sample B (filled triangle). The open circles are reproduced from Ref. [8], where the electrons occupy only the Z valley in a very narrow AlAs QW, and the solid line represents the quantum Monte Carlo prediction of Ref. [12]. The vertical dotted and dashed lines indicate n_V for samples A and B respectively.

where N is the LL index, $\omega_c = eB_\perp/m^*m_e$ is the cyclotron frequency, and Δ_V is the valley splitting. Since our experiment is only sensitive to the field positions of the level crossings, which depend on the relative energy scales in the fan diagram and not on the overall energy scale, we choose the cyclotron energy of the Z valley electrons at $B_\perp = 1$ T as a reference energy. The expression for the LL energies in these units then becomes:

$$E = (N_i + \frac{1}{2})(m_Z^*/m_i^*)B_\perp \pm \frac{1}{4}g_i^*m_Z^*B \pm \frac{h}{4e}n_V \qquad (2)$$

where n_V is the threshold density for minority valley occupation at $B_\perp = 0$ and $i \in \{\mathrm{X}, \mathrm{Z}\}$ is a valley index. We deduce $n_V = 4.2$ x 10^{11} cm^{-2} from the density where the onset of SdH oscillations begins to move to higher $B_\perp$ [the bold trace in Fig. 1(a)]. This value is also confirmed by the Fourier spectra of the Shubnikov-de Haas oscillations in our ρ_{xx} traces, which show additional peaks corresponding to the minority valley above n_V. We use the band mass and g-factor ratios, $m_Z/m_X = 0.45$ and $g_Z/g_X = 1$, despite the presence of interactions; we return to this seemingly questionable assumption later to justify its validity. To complete the fan diagram, we take $g_Z^*m_Z^* = 0.95$ to fit the crossings between opposite spin LLs (same-spin LL crossings are independent of this, given our assumption of equal g-factors) [10]. This value of $g_Z^*m_Z^*$ is less than the measured single-valley value [8] by approximately 20% [Fig. 2], but this difference is comparable to the reduction of g^*m^* reported previously for a 2DES going from single to double valley occupation [11]. The resulting fan diagram is exhibited in Fig. 1(b), and we can see that the spikes at $\nu = 3$, 4, and 5 can reasonably be described as crossings of the Z valley LLs with the lowest LL of the X valley.

According to Fig. 1(b), there should also be a LL crossing occurring in the $\nu = 2$ minimum at $B_\perp = 11.3$ T,

though this is not seen in Fig. 1(a). As the 2DES is heated, this crossing is indeed revealed near the expected field position [Fig. 1(b) inset]. We have measured the activated energy gap at $\nu = 2$, which we call $^2\Delta$ and indicate in Fig. 1(b) by the shaded region, for temperature T, between 0.3 K and 6 K as n is tuned from 5.7 to 2.2 x 10^{11} cm^{-2}. The results are shown in Fig. 1(c). At the $B_\perp = 11.3$ T crossing, $^2\Delta$ is a local minimum, though a finite gap of 7.5 K persists. As n is reduced, $^2\Delta$ increases until $\nu = 2$ reaches the field corresponding to the $\nu = 3$ LL crossing ($B_\perp = 6.7$ T), and decreases thereafter. By introducing an additional energy scale to the system, namely the temperature, we can distinguish between the enhancement of m^* and g^* in principle. To generate our fan diagram, we used $g_Z^* m_Z^* = 0.95$, which is enhanced by a factor of about 2.3 over the band value. In Fig. 1(c), we show the expected gap values if all of this enhancement is assigned to m^* (dotted red) or to g^* (solid blue). The latter agrees more closely with the measured gaps and, while we cannot definitively assign all of the enhancement to g^*, it seems clear that it is responsible for at least some of the overall enhancement. That the agreement persists even below n_V ($B_{\nu=2} = 8.7$ T) suggests that the non-equilibrium population of thermally excited minority-valley electrons continue to affect the overall $g^* m^*$ enhancement. The deviation of the experimental data from the predicted curve at lower n likely results from the increase of $g^* m^*$ that occurs as n is reduced [8, 13] and as the minority valley is further depopulated [11], though the increasing influence of disorder at low n may also play a role.

In order to justify our assumption that the band mass and g-factor ratios apply in the presence of interaction, we have tilted our sample with respect to B. Using equation (2), we can write the expression for the field position of crossings between the Z valley levels and the lowest LL of the X valley:

$$B_{\perp c} = \frac{\frac{h}{e} n_V}{(2N_Z + 1) - \frac{m_Z^*}{m_X^*} + g_Z^* m_Z^* (\frac{g_X^*}{g_Z^*} \pm 1)/2cos(\theta)} \quad (3)$$

where the plus sign in the θ dependent term applies for crossings of LLs with opposite spin and the minus sign for same spin crossings. Figure 1(b) indicates that the odd ν crossings occur between same spin LLs, while the crossings at even ν are between opposite spin LLs. In Fig. 3(a), we see that the the $\nu = 3$ and 5 spike positions remain fixed as we tilt the sample with respect to B. The spike positions for $\nu = 3$, 4, and 5 in sample A are reproduced in Fig. 3(c), plotted as inverse field position vs. $1/\cos(\theta)$. The lines are the predicted behavior based on the parameters used to generate the fan diagram in Fig. 1(b), and the flatness of the $\nu = 3$ and 5 spike positions imply that $g_Z^*/g_X^* = 1$ within an accuracy of better than 1%. We have confirmed this same behavior in sample B with a larger valley splitting ($n_V = 6.2$ x 10^{11} cm^{-2}) [Fig. 3(b) and (d)], and are again able to reproduce the spike positions, here using equal values of g^* for the two valleys, the band mass ratio, and $g_Z^* m_Z^* = 0.92$. The equality of g^* for the two valleys also implies that the band mass ratio applies in our system, since this ratio determines the positions of the same-spin crossings in the fan diagram that are consistent with the spike positions in our data. The fan diagram is not extremely sensitive to the precise value of the mass ratio, however, so the validity of using the band value in the presence of interactions cannot be stated definitively.

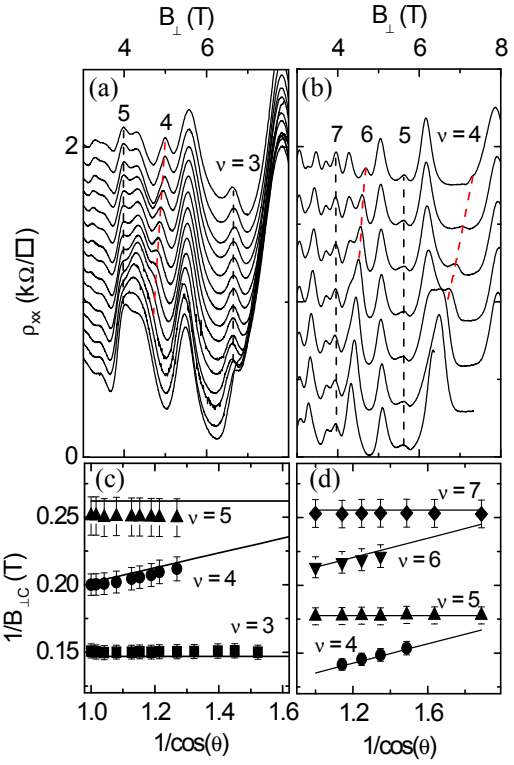

FIG. 3: (color online) (a) ρ_{xx} vs. $B_\perp$ at n = 4.9 x 10^{11} cm^{-2} in sample A as the sample is tilted from $\theta = 0$ (top) to 52^o (bottom) and (b) at n = 6.8 x 10^{11} cm^{-2} in sample B as the sample is tilted from $\theta = 0$ (top) to 58^o (bottom). The positions of the spikes from (a) and (b) plotted as $1/B_{\perp c}$ vs. $1/\cos(\theta)$ are shown in (c) and (d) respectively. The dotted lines in (a) and (b) are guides to the eye, and the solid lines in (c) and (d) are the predicted spike positions based on the 2DES parameters described in the text. Error bars represent the full-width at half-maximum of the spikes.

Several of our observations regarding the characteristic parameters of our 2DES are intriguing in light of recent work. First, it has been shown that $g^* m^*$ is lower in a degenerate, two-valley 2DES than in the single-valley case [11]. Our results indicate that $g^* m^*$ drops significantly with just a modicum of minority valley occupation [Fig. 2]. Second, some measurements performed in Si metal-oxide-semiconductor field-effect transistors (Si-MOSFETs) suggest that the enhancement of $g^* m^*$ is

principally due to m^* enhancement, with g^* never more than a factor of 1.5 above the band value [14]. In our measurements, however, the factor of 2.3 enhancement of g^*m^* appears to be attributable, at least in part, to g^* enhancement, with m^* remaining close to the band value [Fig. 1(c)]. We note, however, that in the range of n that we have measured $^2\Delta$, reported values of g^* and m^* in Si-MOSFETs are both close to the band values with the g^* enhancement even slightly greater than that of m^*. It is only at low n ($\lesssim 2$ x 10^{11} cm^{-2}) that the enhancement of m^* overtakes that of g^* in those measurements [14].

Most surprisingly, our data imply that the electrons in each 2DES are characterized by a *single*, enhanced g^*. We emphasize that this conclusion relies *only* on the lack of angle dependence for the odd ν spike positions and not on any other parameters used to fit those positions. The effect of electron-electron interaction at $B_\perp = 0$ is often characterized by the so-called *interaction parameter*, r_s, which is equal to the ratio of the Coulomb and Fermi energies, the latter of which depends on n and on m^* through the density of states [15]. When the X or Z valleys are singly occupied in QWs with different widths, the interaction enhancement of the band parameters is different owing to their different band effective masses and, hence, different values of r_s [8, 11]. However, when these valleys are occupied in the same QW, as in our samples, the enhancement of g^* appears to be the same for both valleys despite having different masses and very different densities.

Finally, we address the existence of ρ_{xx} spikes at the LL crossings in our measurements. Such ρ_{xx} spikes have been reported previously for single-valley 2DESs in tilted magnetic field at angles where LLs of different spin coincide at the Fermi energy (E_F) [16]. In the case of spin, LLs are expected to be degenerate in the single-particle case at all $B_\perp$ for a particular θ. The existence of persistent gaps and ρ_{xx} spikes are, therefore, quite surprising and have been explained as a consequence quantum Hall ferromagnetism [17, 18] and scattering at boundaries of different spin domains [19]. The situation is somewhat different in the present case, where the LLs are only degenerate at particular values of $B_\perp$ [Fig. 1(b)]. The variation of the energy gap as E_F traverses the localized states over a range of $B_\perp$ could yield spike-like features in ρ_{xx} even in the absence of interaction. On the other hand, it is worth noting that when the X and Z valley LLs are degenerate, interface roughness disorder acts as a random, symmetry-breaking field that favors occupation of the X (Z) valley wherever the QW is locally thicker (thinner), dividing the 2DES into domains and may contribute additional dissipation as the electrons scatter at the domain boundaries.

In summary, we have studied crossings of LLs of a majority Z valley with the lowest LL of the minority X valley in two AlAs QWs with different valley splittings. From the positions of the resistivity spikes and measurements of the energy gap at $\nu = 2$, we find that g^*m^* drops rapidly upon occupation of the minority valley. Of the remaining g^*m^* enhancement, some or all can be attributed to g^* in the n range of our measurements, and, most remarkably, that enhancement of g^* is the same for all electrons despite the occupation of two very different valleys.

We thank the National Science Foundation for financial support and E.P. De Poortere for discussions.

[1] F.F. Fang and P.J. Stiles, Phys. Rev. **174**, 823 (1968).
[2] Two confinement subband systems are an exception, e.g., K. Muraki *et al.*, Phys. Rev. Lett. **87**, 196801 (2001).
[3] H. Momose *et al.*, Physica (Amsterdam) **4E**, 286 (1999).
[4] H.W. van Kesteren *et al.*, Phys. Rev. B **39**, 13426 (1989); K. Maezawa *et al.*, J. Appl. Phys. **71**, 296 (1992).
[5] A.F.W. van de Stadt *et al.*, Surf. Sci. **361/361**, 521 (1996).
[6] Residual, anisotropic stresses in the plane of the 2DES commonly split the X and Y valleys in these systems.
[7] K. Vakili *et al.*, Phys. Rev. Lett. **92**, 186404 (2004).
[8] K. Vakili *et al.*, Phys. Rev. Lett. **92**, 226401 (2004).
[9] Due to the narrow QW width, the next Z-valley confinement subband is not occupied until $n \gtrsim 3$ x 10^{12} cm^{-2}.
[10] Though g^*m^* depends on n in general, we are only concerned with a very narrow range of n where the spikes fall at integer ν, and are thus justified in using a constant value to generate our fan diagram.
[11] Y.P. Shkolnikov *et al.*, Phys. Rev. Lett. **92**, 246804 (2004).
[12] C. Attaccalite *et al.*, Phys. Rev. Lett. **88**, 256601 (2002).
[13] g^*m^* increases by about 35% between $n = 2.1$ and 5.7 x 10^{11} cm^{-2}, though most of the increase happens towards the lower n range. This would tend to reduce the size of the predictions for the gap at $\nu = 2$ shown in Fig. 1(c).
[14] A.A. Shashkin *et al.*, Phys. Rev. B **66**, 073303 (2002).
[15] Measurements in AlAs QWs show no significant dependence of g^*m^* on $B_\perp$ (e.g., Ref. [8]), so r_s still parameterizes g^*m^* enhancement for $B_\perp > 0$.
[16] E.P. De Poortere *et al.*, Science **290**, 1546 (2000).
[17] T. Jungwirth *et al.*, Phys. Rev. Lett. **81**, 2328 (1998).
[18] T. Jungwirth and A.H. MacDonald, Phys. Rev. B **63**, 035305 (2000).
[19] T. Jungwirth and A.H. MacDonald, Phys. Rev. Lett. **87**, 216801 (2001).
[20] Y.P. Shkolnikov *et al.*, Phys. Rev. Lett. **89**, 226805 (2002); V.S. Khrapai *et al.*, Phys. Rev. B **67**, 113305 (2003); Y.P. Shkolnikov *et al.*, Phys. Rev. Lett. **95**, 0666809 (2005).
[21] P.C. Klipstein, Semicond. Semimet. **55**, 45 (1998).